

GEOPHYSICS Bright Spots

COORDINATED BY CHRISTINE KROHN

This is my last time coordinating the Bright Spots column. The new coordinator will be Jyoti Behura. This has been an enriching assignment. I had the opportunity to read many interesting papers covering the breadth of geophysics research. The papers were nominated by the assistant editors of GEOPHYSICS. They do the hard work by shepherding submissions through the review process and nominating a select number to be highlighted.

Inversion of CSEM with MT data

In “Marine controlled-source electromagnetic of the Scarborough gas field — Part 3: Multicomponent 2D magnetotelluric/controlled-source electromagnetic inversions,” Constable et al. investigate the potential for improved resolution with the inclusion of other electromagnetic data sets in the inversion of controlled-source electromagnetic (CSEM) data. Field data for the study were collected over the Scarborough gas field on the northwest shelf of Australia. Marine CSEM data have become a valuable component of offshore exploration, particularly in the hydrocarbon sector. The standard data set consists of measurements at the seafloor of the horizontal electric field generated by a horizontal deep-towed electric transmitter. The sensitivity of these data to thin subhorizontal resistors makes them useful for detection and delineation of oil and gas fields. In this paper, the authors evaluate the advantages of measuring the horizontal magnetic field, vertical electric field, and magnetotelluric (MT) data. MT data utilize natural variations in earth’s magnetic field as the source instead of using an active transmitter. The horizontal magnetic field response is similar to that of the horizontal electric field and does little to improve resolution. Vertical electric field data are subject to more noise than horizontal field data, but improve resolution, especially when inverted on their own. The biggest improvement, however, comes from including MT data with standard CSEM data. As shown in Figure 1, the reservoir response is smeared into the response of a resistive basement when CSEM data are used alone. The addition of MT data separates the two responses. MT data can be collected using the same instruments that collect CSEM data, so this improvement comes at little additional cost. Adding vertical electric field data contributes to additional improvements, helping to separate the reservoir from an overlying resistive siltstone, but at some additional cost in acquisition logistics. These results should guide the design of future CSEM data collection.

FWI using a CNN

A convolutional neural network (CNN) is commonly implemented to generate or to classify models based on a training data set with many samples. In their paper “Parametric convolutional

neural network-domain full-waveform inversion,” Wu and McMechan use CNN as a regularization tool for full-waveform inversion (FWI). They update the CNN weights to iteratively reparameterize and regularize a velocity model to minimize seismic data residuals. CNN-domain FWI includes two steps: CNN pretraining (reparameterization) and CNN-domain inversion (regularization). In CNN pretraining, reparameterization of the velocity model in the CNN domain enables CNN hidden layers to automatically capture salient features (e.g., locations and shapes of salt bodies or strong reflectors) from the starting model as prior information with multiscale resolution. Most FWI algorithms are not able to accurately handle salt or other high-contrast interfaces. CNN-domain inversion is similar to conventional FWI, except FWI automatically constrains the updates of CNN weights by regularization to these captured features in the CNN-generated velocity model. CNN-domain FWI relies on prior information in the starting velocity model. The more useful the prior information (e.g., locations and shapes of features) included in the starting model is, the better the velocity model inverted by CNN-domain FWI will be. Figure 2 compares the velocity model inverted by conventional and CNN-domain FWI using the Sigsbee velocity model.

AVO inversion with a quasi-elastic wave equation

Early intuitive understanding of elastic amplitude-variation-with-offset (AVO) effects was provided by linearization of the elastic parameters in Zoeppritz equations, such as Shuey’s or Fatti’s approximations. This was largely responsible for the widespread use of reflectivity-based AVO techniques. Feng and Schuster present the quasi-elastic wave equation as a function of the pressure variable by linearizing the elastic wave equation under the first-order Born approximation in their paper, “True-amplitude linearized waveform inversion with the quasi-elastic wave equation.” The quasi-elastic wave equation can model

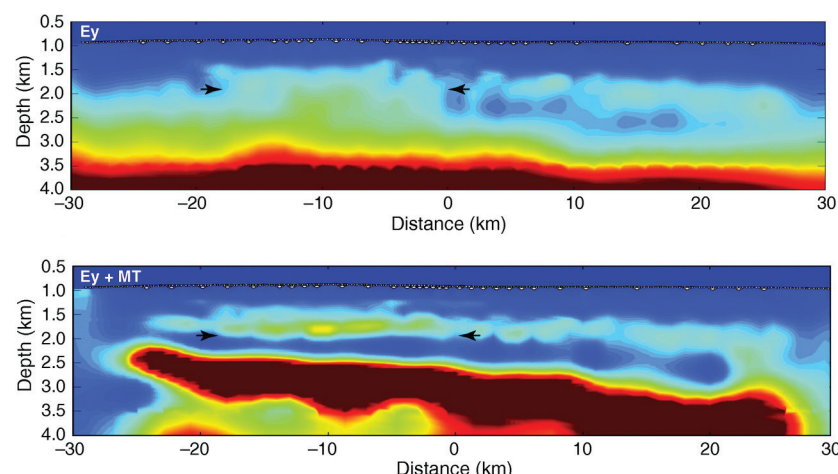


Figure 1. (Figures 9a and 11a from Constable et al.) Jointly inverting MT data along with the Ey component from CSEM data improves the ability to separately resolve the basement and reservoir when compared with inversion of Ey alone. The arrows indicate the edges of the gas reservoir based on the seismic data.

PP reflections with accurate AVO effects using only the acoustic wave equation. The equation allows the inversion of perturbations of shear modulus or S-wave impedance using acoustic least-squares reverse time migration (LSRTM). The method was tested with three different synthetic data sets and a Gulf of Mexico field example (Figure 3). Compared with the conventional reflectivity-based AVO technique, linearized waveform inversion with the quasi-elastic wave equation does not require careful data processing for estimating reflectivity values for analytical analyses of elastic parameters. Compared with conventional acoustic LSRTM, it properly accounts for the AVO effects for

PP reflections, provides images with a wider bandwidth and fewer artifacts, and gives a reliable estimate of P- and S-wave impedances. Compared with conventional elastic FWI, it can result in computational savings of more than an order of magnitude, because only solutions to the acoustic-like wave equations are required.

Microseismicity caused by water injection

In “Microseismicity caused by injection of water in a gas-saturated reservoir,” Macias et al. analyze the effects of gas and water saturation and reservoir properties on the microseismic

event distribution caused by water injection into a low-permeability gas reservoir. Rock stresses, initial water saturation, and the presence of natural fractures influence the time-spatial distribution of microseismic sources. The novel aspect of the approach is the interaction between fluid phases. Rock breaking generates microseismic events as well as variations in the reservoir properties, which are updated during injection. Reservoir initial gas saturation, rock stress, and the presence of natural fractures are taken into account. The results are presented as maps of the events as well as their temporal distribution. The authors highlight the importance of using two fluid phases and accurate reservoir information to estimate the distribution of microseismic events.

FWI for crosshole GPR

Klotzsche et al. review performing FWI on ground-penetrating radar (GPR) data in “Review of crosshole ground-penetrating radar full-waveform inversion of experimental data: Recent developments, challenges, and pitfalls.” Theoretical papers have shown the potential of GPR FWI to resolve heterogeneous small-scale layers and spatial variabilities of soil properties, which can have a large impact on flow and transport processes in the earth’s critical zone. Applying crosshole GPR FWI to experimental data is challenging and requires a careful choice of inversion parameters and careful use of preprocessing steps. Over the last decade, applications to experimental data have matured, making GPR FWI an established approach for improving resolution. This paper provides a baseline and guide for the application of GPR FWI to field data. The authors

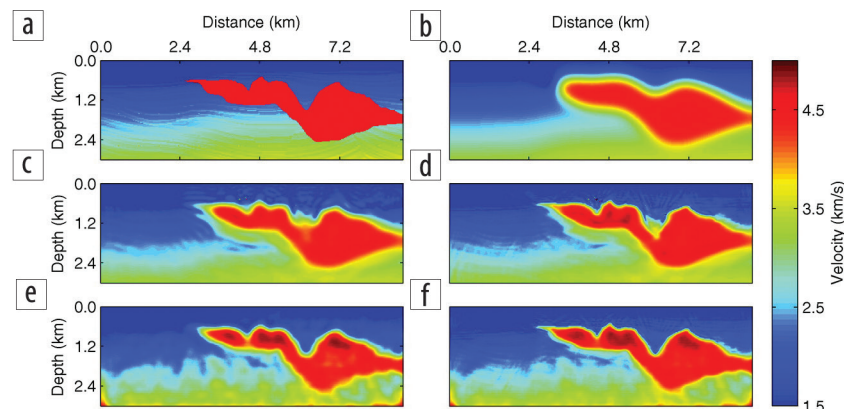


Figure 2. (Figure 8 from Wu and McMechan.) Comparison of the Sigsbee velocity models. (a) True velocity model. (b) Initial velocity model. (c) Conventional FWI after pass 1. (d) Conventional FWI after pass 2. (e) CNN-domain FWI after pass 1. (f) CNN-domain FWI after pass 2. The final CNN-domain FWI velocity model has a root-mean-square velocity residual of 9.5% compared to 13.7% for conventional FWI. The major difference is near the boundaries of the salt.

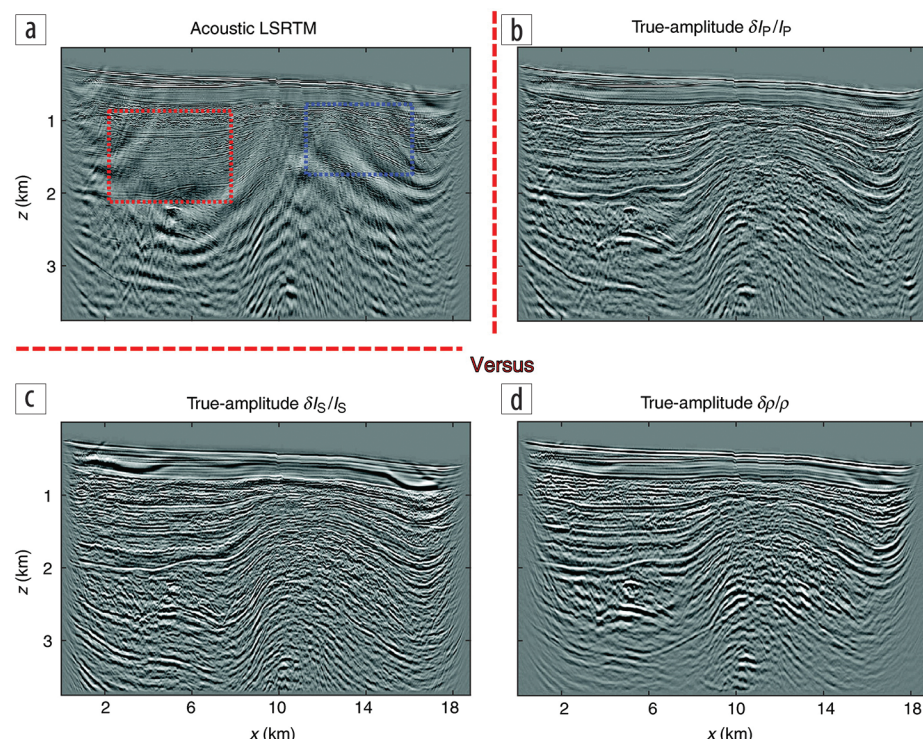


Figure 3. (Figure 20 from Feng and Schuster.) Shown for the Gulf of Mexico field data are the (a) conventional LSRTM image and true-amplitude linearized inversion for perturbations for (b) P-impedance, (c) S-impedance, and (d) density. The images for $\delta I_p/I_p$ are more continuous and distinct, with wider bandwidth and fewer artifacts. The $\delta I_s/I_s$ and $\delta \rho/\rho$ images are structurally similar but have narrower bandwidth.

illustrate the necessary steps for obtaining reliable and reproducible high-resolution images of permittivity and electrical conductivity. Examples generated using an experimental crosshole GPR data set from a test site in Switzerland illustrate challenges, showing the output for different FWI development steps and possible pitfalls. For example, the authors point out the importance of a correct time-zero correction of the data, estimation of the effective source wavelet, and effect of the choice of starting models (Figure 4). Reliability of the FWI results is investigated by analyzing fit of the measured and modeled traces, the remaining gradients of the final models, and validating the results with independently measured logging data. The authors hope that the paper will enable greater use of crosshole GPR FWI for different applications.

Viscoacoustic anisotropic wave equations

Seismic wave propagation in the earth is affected by attenuation and anisotropy due to the nature of gravity-induced sedimentation, fluid-filled fractures, regional stresses, etc. Incorporating attenuation and anisotropy into the wave equation may improve the image quality of wave-equation-based imaging methods. In their paper “Viscoacoustic anisotropic wave equations,” Hao and Alkhalifah propose a general representation of the scalar and vector viscoacoustic wave equations for orthorhombic anisotropy, which is flexible for multiple viscoacoustic models. Their general form allows for transformation to the wave equations in differential form for a few classic viscoacoustic models. This can be done predictably for more complicated models in a similar way. These wave equations in differential form are efficiently solvable with the aid of existing numerical methods, such as finite difference, finite element, spectral element, etc. Compared with classic viscoelastic anisotropic wave equations, their viscoacoustic wave equations involve fewer parameters for characterizing the P-wave velocity and attenuation anisotropies and are more suitable for practical applications. They also derive asymptotic point-source radiation, which provides insight into the role

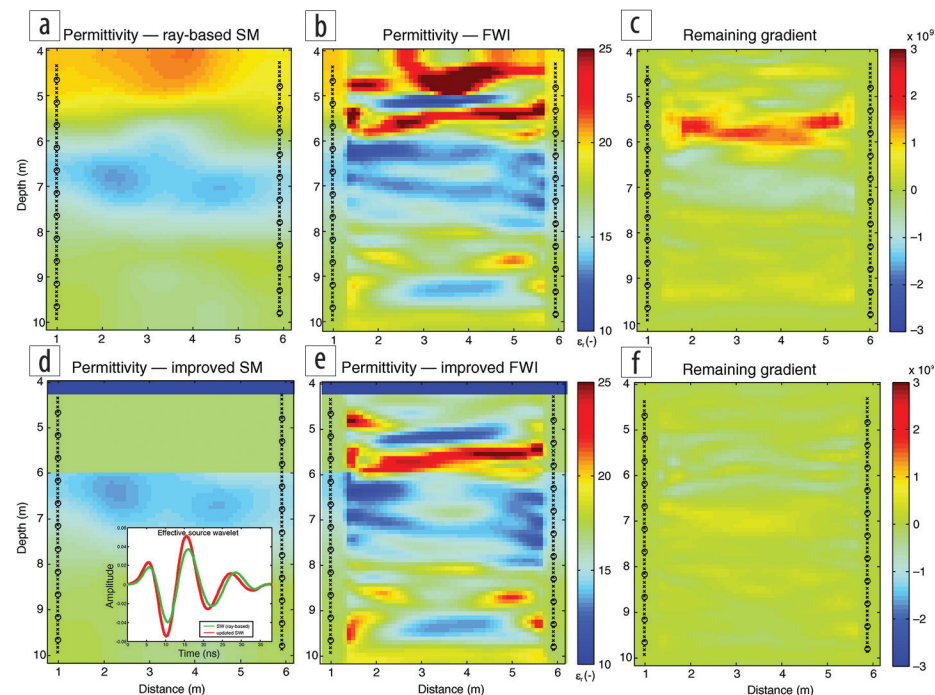


Figure 4. (Figure 4 from Klotzsche et al.) Illustration of the starting model problem. Permittivity for (a) ray-based inversion results, (b) corresponding FWI, and (c) remaining gradients. These can be compared to (d) an improved starting model, (e) FWI, and (f) gradient. The inset in (d) shows the estimated effective source wavelets for the ray-based (green) and improved (red) starting models.

that attenuation plays with wave amplitudes. Their point-source radiation formula reveals that the phase and attenuation of seismic waves in a homogeneous viscoacoustic anisotropic medium can be described by the real and imaginary parts of complex traveltimes. In the inhomogeneous case, the complex traveltimes can be obtained by numerically solving attenuating eikonal equations. The point-source radiation analysis demonstrates: (1) the attenuation-dominant component is given by a decay in wave amplitudes since it barely affects the arrival times; (2) attenuation anisotropy causes such a decay in wave amplitudes that vary with direction; and (3) velocity dispersion and frequency-dependent attenuation stretch and distort the waveforms. Overall, their viscoacoustic wave equations provide a chance to realize the forward and inverse modeling and imaging problems in a practical framework, which does not require shear-wave velocity, attenuation, or anisotropy values.

Other papers nominated by the editors

- Das et al. — “Convolutional neural network for seismic impedance inversion” **TL**